California Solar Initiative

RD&D: Research, Development, Demonstration and Deployment Program

Final Project Report:

West Village Energy Initiative APPENDIX B:

Task 1 Demo 2 Single Family Home Energy Storage

Grantee:

University of California, Davis

Energy Institute

July, 2015

www.CalSolarResearch.ca.gov

PREPARED BY

University of California, Davis
Energy Institute

UC Davis Energy Institute
1 Shields Avenue
Davis, CA 95616
530-752-4909

University of California, Davis
Office of Environmental
Stewardship and
Sustainability

436 Mrak Hall
University of California, Davis

Principal Investigator:
A. Sidney England
asengland @ ucdavis.edu

Project Partners:
E3
DEG
General Electric

PREPARED FOR

California Public Utilities Commission
California Solar Initiative: Research, Development, Demonstration, and Deployment Program

CSI RD&D PROGRAM MANAGER

Program Manager:
Smita Gupta
Smita.Gupta@itron.com

Project Manager:
Smita Gupta
Smita.Gupta@itron.com

Additional information and links to project related documents can be found at

DISCLAIMER

"Any opinions, findings, and conclusions or recommendations expressed in this material are those of the author(s) and do not necessarily reflect the views of the CPUC, Itron, Inc. or the CSI RD&D Program."

http://www.calsolarresearch.ca.gov/Funded-Projects/

Preface

The goal of the California Solar Initiative (CSI) Research, Development, Demonstration, and Deployment (RD&D) Program is to foster a sustainable and self-supporting customer-sited solar market. To achieve this, the California Legislature authorized the California Public Utilities Commission (CPUC) to allocate **$50 million** of the CSI budget to an RD&D program. Strategically, the RD&D program seeks to leverage cost-sharing funds from other state, federal and private research entities, and targets activities across these four stages:

- Grid integration, storage, and metering: 50-65%
- Production technologies: 10-25%
- Business development and deployment: 10-20%
- Integration of energy efficiency, demand response, and storage with photovoltaics (PV)

There are seven key principles that guide the CSI RD&D Program:

1. **Improve the economics of solar technologies** by reducing technology costs and increasing system performance;
2. **Focus on issues that directly benefit California**, and that may not be funded by others;
3. **Fill knowledge gaps** to enable successful, wide-scale deployment of solar distributed generation technologies;
4. **Overcome significant barriers** to technology adoption;
5. **Take advantage of California's wealth of data** from past, current, and future installations to fulfill the above;
6. **Provide bridge funding** to help promising solar technologies transition from a pre-commercial state to full commercial viability; and
7. **Support efforts to address the integration of distributed solar power into the grid** in order to maximize its value to California ratepayers.

For more information about the CSI RD&D Program, please visit the program web site at www.calsolarresearch.ca.gov.

Abstract

This paper presented the use of second life battery pack in a smart grid-tie photovoltaic battery energy system. The system was developed for a single family household integrating PV array, second life battery pack, grid back feeding, and plug-in hybrid electric vehicle charging station. A battery pack was assembled using retired vehicle traction battery, with 9 cells in each parallel bank, 15 banks in a series, featuring 48 V nominal voltages and 12 kWh nominal capacities. Limited by the weakest bank in the pack, the second life battery pack has accessible capacity of 10 kWh, 58% of its original condition. Battery management was applied to handle the imbalance and ensure the safety operation limits of the battery pack. Energy flow controller was established to optimize the energy harvest from PV while minimize the grid dependence. An information network was constructed to acquire data from battery, PV and appliances and major inverters using Zigbee and wireless qualified devices. The presented system achieved utilization of used vehicle traction battery for second round of application, optimization of solar energy harvest and supporting electric vehicle charging.

Acknowledgements

The research team gratefully acknowledge the support of California Solar Initiative (CSI) in funding this research project, and the support of Itron, UC Davis PHEV Center, SMA Inc., Wireless Glue Network in helping the system development.

Executive Summary

Table of Contents

Abstract 2
Acknowledgements 3
Executive Summary 3
Table of Contents 4
List of Tables 4
List of Figures 5
Nomenclature (Table) 6
Introduction 6
Methods 8
System Design and Functional Specification 8
Battery Pack Design 9
Battery Management System (BMS) Design 13
Energy Management Algorithm 16
System Design Document, Installation and Commissioning 19
Remote Data Acquisition and Monitoring 21
Results and Discussion 24
Conclusions 27
Recommendations 28
References 29
Appendix 30
Subheading 30

List of Tables

Table 1: Comparisonn of candidates for stationary energy storage 7
Table 2. Energy management decision making table. 17
Table 3. List of data logging server 23
Table 4. System operation statistics. 25
Table 5: Summary of state-state model for the worst battery bank 31
Table 6: Summary of state space model for the difference between the worst banks and the rest of the banks 32
Table 7: Summary of computation steps for Extended Kalman Filter. 32

List of Figures

Figure 1 Second use of vehicle traction battery as stationary energy storage 8
Figure 2 System diagram 9
Figure 3 Footsteps of battery pack design 10
Figure 4 Fifteen battery banks with various useable capacities 10
Figure 5 Assembled battery pack: (a) design diagram, (b) battery balancing box, (c) battery box 12
Figure 6: On-line battery voltage monitoring during battery pack charge and discharge 13
Figure 7 Flow chart of multiple time scales battery state estimation algorithm 14
Figure 8 Diagram of multiple time scales battery state estimation algorithm 15
Figure 9: On-line battery SoC estimation during battery pack charge and discharge 15
Figure 10: Identified battery pack SoC and SoH imbalance during system operation 16
Figure 11: System operation simulation under good solar harvesting weather 18
Figure 12: System operation simulation under poor solar harvesting weather 18
Figure 13: Design document – battery pack 19
Figure 14: Design document – rooftop PV/PVT array 20
Figure 15: Design document– the overall energy system 20
Figure 16: Photo of installed smart-grid PV battery system 21
Figure 17: Diagram of system information network 22
Figure 18: Screen shot of web based data server: top, sma webbox;middle, obvius smart panel; bottom, TiGo system 23
Figure 19: Screen shot of web based live data panel 24
Figure 20. Sample of system operation on 12/01/2013 26
Figure 21. Sample of system operation on 12/10/2013 27

Nomenclature (Table)

Name	Property
PHEV	Plug-in hybrid electric vehicle
EV	Electric vehicle
DoD	Depth of discharge
SoC	State-of-charge
PV	Photovoltaic
PVT	Photovoltaic thermal
ICE	Internal combustion engine
MPPT	Maximum power point tracking
BMS	Battery management system
SoH	State-of-health
EKF	Extended Kalman Filter
PVA	Parameter varying approach

Introduction

Second life batteries are batteries retired from their first application in plug-in hybrid electric vehicles (PHEV) or electric vehicles (EV) and repurposed for a second, typically lower performance application. The reduced performance application is generally required due to the imminent degradation that happens to batteries during their first application. According to the US Advanced Battery Consortium (USABC) standard for EV batteries, a battery cell has reached its end of life when the cell capacity has dropped below 80% of the rated capacity or the power density becomes less than 80% of the rated power density at 80% depth of discharge (DoD)[1]. For PHEVs, the impact of battery pack performance degradation is less significant, since the performance degradation of the battery pack due to aging can be compensated by the internal combustion engine (ICE). As a result, a PHEV battery may degrade more than the USABC standard specifies while still being able to provide value in an automotive application. Consequently, it is expected that battery cells with 80%, or less, of the rated capacity will be retired from PHEV/EV applications and will be available in the second life market. As PHEVs and EVs gain popularity the number of aged vehicle batteries will increase, posing recycling issues and making second life applications more attractive. Second use of lithium-ion traction battery applications is an applicable approach to extend the useful battery life. This aids in conserving resources and reducing environmental impacts, and is expected to have significant market potential as lithium-ion battery packs are beginning mass production for transportation use[2,3]. A second life battery pack, when properly sized, is able to deliver equivalent performance as a new battery pack, but at a larger volume and lower cost. Another important

feature of a second life battery pack is, when cells of varying quantities of degradation are assembled together, the performance of the whole pack is governed by the weakest bank. The increased likelihood of battery bank capacity imbalance in second life battery packs has increases the risk of over voltage and/or over current within the pack, and therefore requires a well-integrated battery management system[4-9].

Battery Types	Price per kWh	Service Life	Issues?
Lithium Batteries	~600	27000+ cycles*	High price;
Lead Acid Batteries	~330	~2000 cycles**	Short life
2nd Life Lithium Batteries	~120***	~5 years****	Low power density; Cell imbalance;
Pumped Hydro	<100	>20 years	Suitable for big power rating applications;

*Test performed by Sandia National Lab on a LiFePO cell with 0.6C Utility PSOC cycle

**Test performed by Sandia National Lab on AGM VRLA batteries with 1C Utility PSOC cycle. Note that carbon enhanced VRLA batteries have cycle life performance compatible to lithium battery at lower energy density

***a discount of 80% is expected for second life battery price

****Test performed in our lab on a second life LiFePO cell with 1C cycle resulting the cell degrading from original 80% capacity to 64% capacity

Table 1: Comparisonn of candidates for stationary energy storage

As energy generation shifts from fossil fuels to alternative sources, energy storage will become an important component for grid stability and peak shifting, due to the improperly matched peak production of renewables versus grid demand [10-17]. Over the years, lithium ion battery applications have expanded from mobile electronics to automotive and aerospace. Popular candidates for battery stationary energy storage includes lithium batteries, lead acid batteries, flowing electrolyte batteries or sodium-beta high temperature batteries. The flowing electrolyte batteries and the sodium-beta high temperature batteries contain toxic or highly corrosive materials, and require advanced infrastructures to provide thermal management [3]. Several storage candidates were compared in Table 1. Lithium batteries will serve as a promising candidate for grid storage if not for its high unit price [18]. The dominant grid energy storage approach now is pumped hydro, which accounts for 99% of grid storage systems operated in the U.S. With less than US$100 per kWh unit price, long service life and 70% or higher efficiency, the pumped hydro seems to be the optimal choice when it comes to large scale energy storage. However, the advanced smart grid is also seeking energy storage solutions that are localized and more responsive to perform grid response and dynamic peak shifting. In this case, smaller scale battery systems have the advantage of handling varying loads and can be easily implemented at any location with simple infrastructure. As a result, the reduced cost of second life lithium ion batteries is appealing to stationary energy storage applications since they may be effectively implemented in small scale applications to deliver high localized fidelity for demand response.

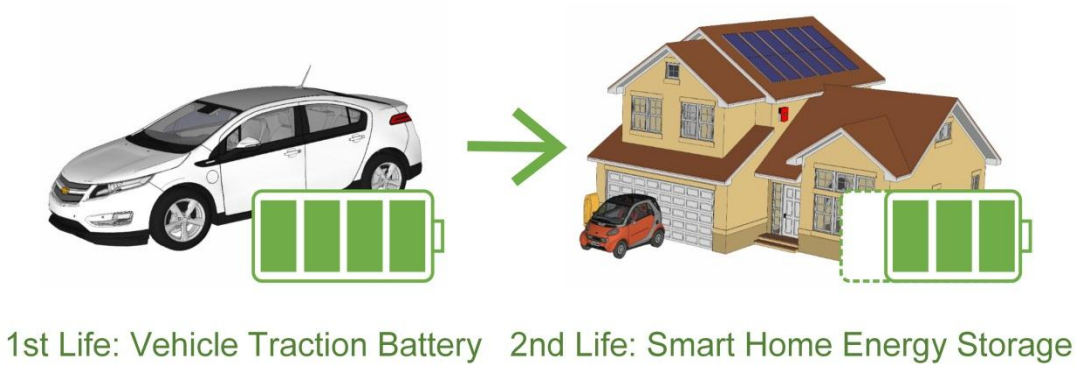

Figure 1. Second use of vehicle traction battery as stationary energy storage.

This report presents the development and preliminary use of a second life battery pack in a Smart Grid-tied Photovoltaic Battery Energy System. The system was developed for a single family household which integrates the use of a PV array, grid back feeding, battery storage and a PHEV charging station. The following tasks were accomplished in the system development phase: 1) battery pack integration into the energy system; 2) application of proper management to the battery pack; 3) design of an energy management algorithm which considers a simple case for grid response, PV energy harvest, house demand and battery safety; 4) develop an information network for energy management and data acquisition. As illustrated in the Figure 1, the project is proposed to apply a second round use of vehicle traction batteries as stationary energy storage into a PV array and vehicle charging equipped smart house.

Methods

System Design and Functional Specification

The system was designed to enable the following functions: (1) support the energy demand of a single family household using both utility power and PV panels; (2) optimize grid dependence using battery storage; (3) enable grid back feeding during peak utility cost; (4) charge a PHEV using a level II charging station.

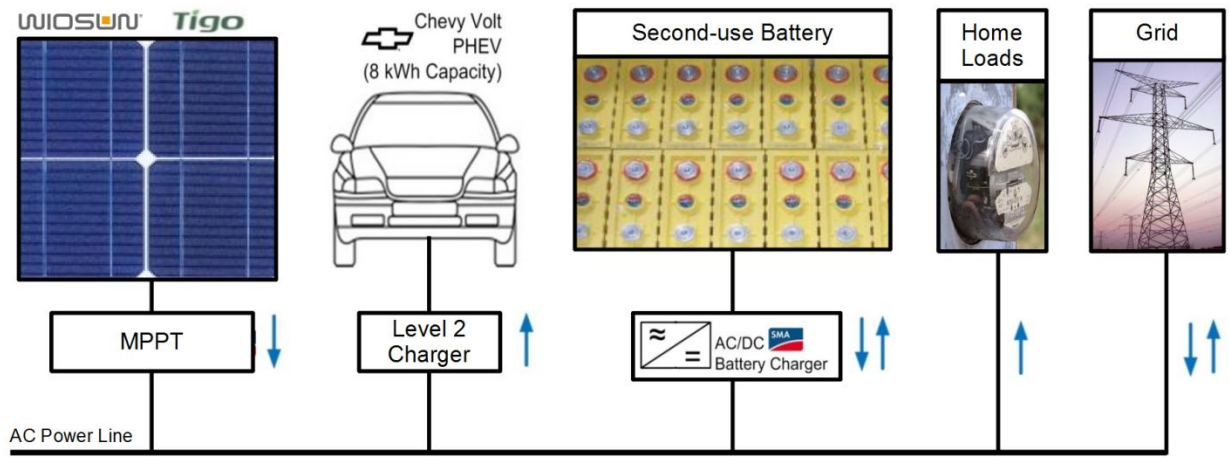

Figure 2. System diagram.

Figure 2 shows a diagram of the system components. One PV string consists of 12 panels, each featuring 180W of rated power. In series this string provides a 2.16kW nominal power output and was installed on a south facing rooftop at the project house. Each panel was connected to a DC-DC converter with maximum power point tracking (MPPT) to optimize the output of each PV module (TiGo sytem®). The entire array was then connected to a DC-AC MPPT converter (SMA system®) to convert the DC solar power into AC power for connecting to the main home power bus. The maximum power tracking provides a high solar energy harvesting efficiency considering irradiance fluctuation and partial shading. A battery pack serves as energy storage of the system and uses a bi-directional AC-DC converter to input and output energy from/to the main power bus. The battery pack was assembled using 135 units of second life LiFePO4 based cells. The batteries were originally manufactured with a capacity of 40Ah, however, after years of service as vehicle traction batteries, these second life batteries have a remaining capacity between 20-30Ah. The battery pack has 9 cells in each parallel bank and 15 banks in series, which provide 48V nominal and 12kWh of nominal energy capacity. Limited by the weakest bank in the pack, the second life battery pack has a total accessible capacity of 10kWh, or 58% of the original condition. The battery pack is controlled to absorb excess energy production from the PV during off-peak hours, and partially support the house load during peak times. Additionally, the control algorithm is programmed to maintain a high level of charge in the battery to enable use as a backup power source. A vehicle charging station will be installed to provide Level II charge to a PHEV. The vehicle will be charged daily with an estimated energy requirement that may vary between 2 to 8kWh. Energy flow from the grid is monitored via a smart meter. The total rated power is 10kW for the interconnected system.

Battery Pack Design

One of the novelties of this project is that a second life battery pack has been used. We received the used battery cells from two different suppliers with different usage histories. As a result, the cells have different levels of state-of-health (SoH). In order to assemble them together to form a functioning battery pack, three design steps were taken to ensure reliable performance of the pack as shown in Figure 3. Stage 1 involved testing the cell conditions, wiring battery cells

together to form a battery pack, installing electrical energy management components, and validating the functionality of the multiple redundant safety features of the battery pack; Stage 2 involved manufacturing the battery box, and assembly of the full battery pack; Stage 3 involved installing the battery pack in the house, and performing preliminary testing.

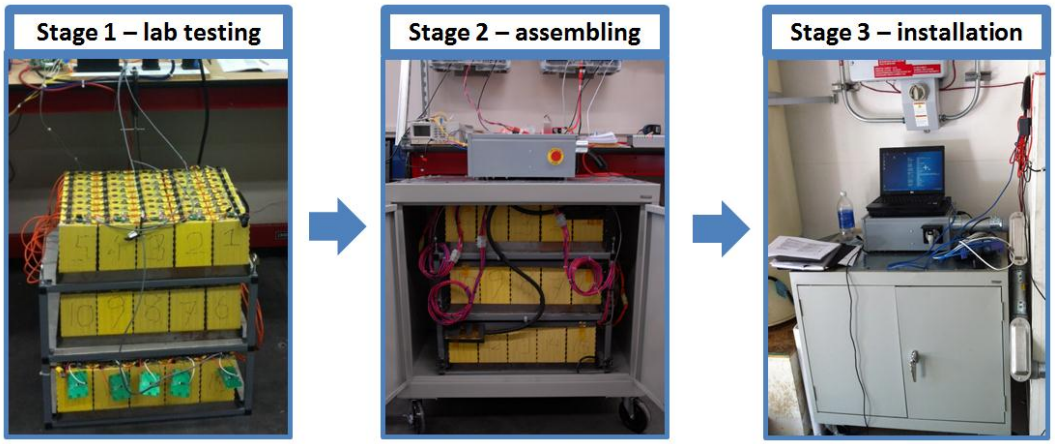

Figure 3. Process of battery pack design.

In stage 1, prior to assembling the battery pack, 15 battery banks were individually tested to quantify their capacity. As shown in Figure 4 the 15 banks possess different useable capacities, the best battery bank being #13, which has a useable capacity of 328Ah, while the worst battery bank is #14, providing 287Ah.

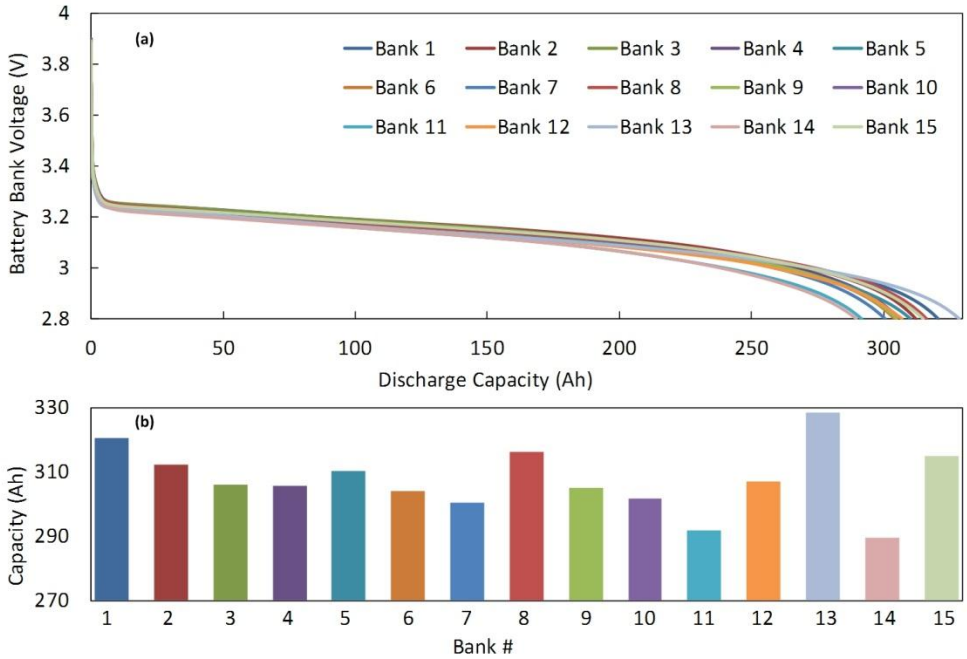

Figure 4. Fifteen battery banks with various useable capacities.

Fourteen banks were wired to form a battery pack. Each cell was wired using a copper bar on the negative terminal and a fusible link on the positive terminal. This approach will isolate an individual cell in the case of a hard short circuit. A detailed wiring illustration can be found in Figure 5(a). At the terminal of the 15 battery banks a BMS slave board was installed and each board measures the battery bank voltage as well as the slave board temperature. A current sensor was installed at the terminal of the battery pack to measure the current in and out of the battery pack. Temperature, current and voltage measurements are converted to digital signals and sent back to the BMS master via line 2 as illustrated in Figure 5(a). Safety limits were set such that if any of the banks are observed to have an abnormal measurement (temperature higher than 80°C, current higher than 150A, and voltage out of 2.8~3.65V range), the contactors (high-powered relays) will open in order to shut off the battery pack from the external source or load via line 3 as illustrated in Figure 5(a). Functions of each individual balancing board and the relay were tested at stage 1. The balancing board will turn on when the attached bank has a voltage higher than the rest of battery pack and approaches full charge. These boards may at most dissipate energy at the rate of 2A in the form of resistive heating via line 4 as illustrated in Figure 5(a). A 48 to 12V DC-DC was used to power the battery management appliances via line 8 and 9 as illustrated in Figure 5(a). This is powered directly from the battery, such that it will run even if the contactors are opened, in order to maintain fulltime control. With this architecture care must be taken to ensure that the BMS does not accidentally over-discharge the battery.

The battery pack was controlled via closed loop feedback. In Figure 5(a) the BMS master board collects essential measurements of the battery pack and sends them to BMS via line 6. The BMS estimates the battery SoC and SoH. Based on the battery SoC, PV power output, and house power load, the BMS generates a battery control signal and sends this to the inverter via line 7. The inverter then controls the battery pack current in/out of the system via line 1. The BMS was custom developed by the research team and acts as the 'brain'/high-level controller of the battery. Detailed descriptions of the battery state estimator design and energy management algorithm design are documented in the following two chapters.

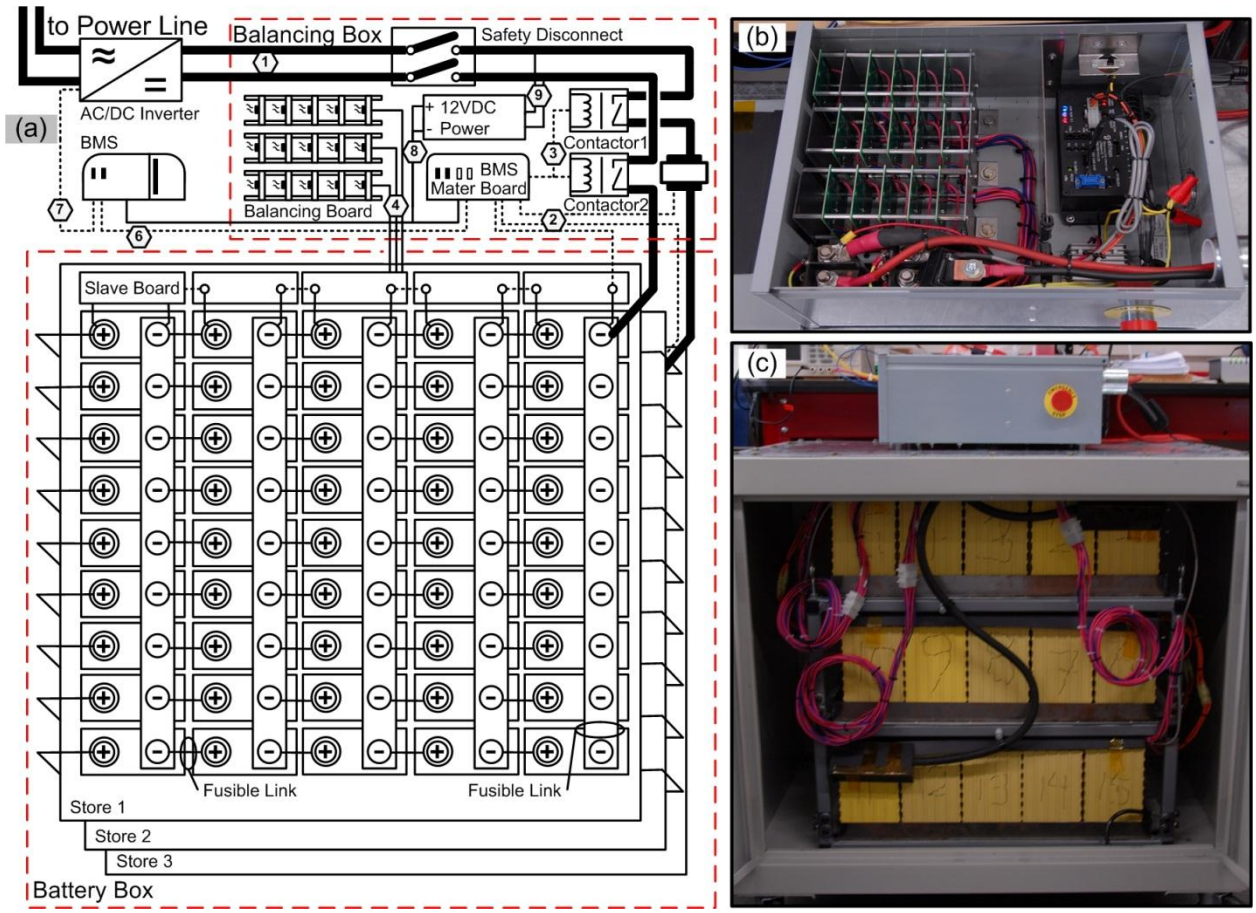

Figure 5. Assembled battery pack: (a) design diagram, (b) battery balancing box, (c) battery box.

Stage 2 is mainly the battery assembly phase. A battery box was custom designed to fulfill all design aspects and fits the battery pack in the designated space within the project house. First, a rack was manufactured to locate the battery pack in three layers. As illustrated in Figure 5(a)(c), each layer contains five battery banks and connects to the neighboring layer via fusible link wires. On top of each battery layer, a sheet of isolation plastic was applied to avoid short circuiting. ITW Formex® plastic was used as this meets UL 94-V0 flammability ratings in high-voltage applications. The rack altogether with the battery pack was installed in the battery box as a single unit via a pass-through placed at the top of the enclosure. A sheet-metal cover was then bolted on the top of the battery box with a small pass-through that allowed for the power and communication cables from the battery pack to enter the balancing box. As shown in Figure 5(b) the balancing box contains: 15 battery balancing boards, two contactors continuously rated at 150A, the BMS master board, a DC power supply, and a manual power cut-off switch. The heat sources (balancing boards and relays) are installed in the balancing box, thus isolating their heat output away from the batteries. This feature effectively prevents the battery pack from overheating while balancing. In stage 3, the fully tested and assembled battery pack was shipped to the project house. The contractors installed the battery pack with the rest of the system, some tests were performed on- site to ensure all the functionality of the system and that communication between the BMS and the rest of the system was established. Figure 6 shows the battery voltage measurements of the battery pack during a simple charge and discharge after

the battery pack was installed in the house. After that, the battery pack was fully functioning in the house as the energy storage system.

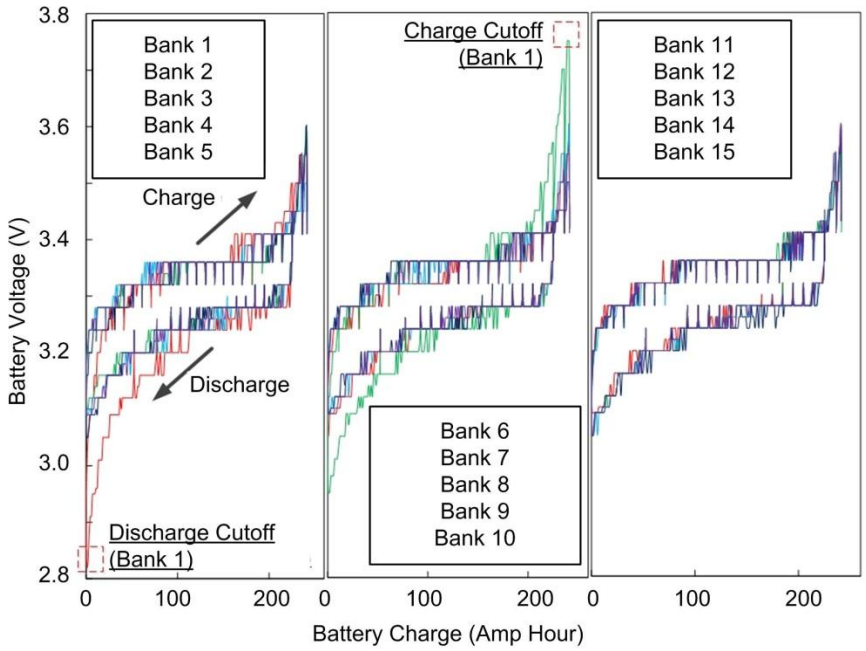

Figure 6. On-line battery voltage monitoring during battery pack charge and discharge.

We successfully delivered a second life battery pack design from scratch. It validates that used vehicle traction batteries, with proper testing and reconfiguration, can be integrated to create a functioning battery pack to be used in a stationary energy storage application.

Battery Management System (BMS) Design

Among all the reconfiguration effort to design a second life battery pack, the most important task is custom design an estimator that is able to accurately estimate both the SoC and SoH of all 15 battery banks while the system is under operation. SoC and SoH of the battery pack, which during dynamic operation may not be directly measured, are important battery state variables that are needed for battery management. For this battery pack, a multiple-time-scales worst-difference estimation approach was applied for SoC and SoH estimation.

In general, the proposed scheme identifies the worst battery bank in the pack, which has the smallest capacity, and allocates the available computing resources to provide close monitoring SoC and SoH of the worst bank. As for the rest of the banks, the scheme estimates their SoC and SoH by comparing them to the worst bank, significantly reducing computing resource demands. Figure 7 summarizes the flow chart of the scheme, which includes all the steps that are executed for a complete estimation cycle. It starts with initializing the state values, parameters and data buffers to be used in the scheme (step 1). At the beginning of the computing iteration (step 2), a fresh set of battery measurements are taken. Based on the knowledge of the battery pack, one bank will then be identified to be the worst battery bank (i.e. the lowest capacity). The SoH estimator then optimizes the battery capacity value of all 15 banks (step 3 to 7), at a frequency of Time Scale 4, using a varying parameter optimization approach.

The SoH estimator also optimizes the battery internal resistance value of the worst bank based on cached measurement data (step 8 to 10), and this is processed at Time Scale 3. An Extended Kalman filter (EKF) was then applied to estimate the SoC of the worst bank (step 11,12) at Time Scale 1. Then, another EKF was applied to estimate the SoC difference between the worst bank and the rest of the banks at Time Scale 2 (step 13, 14). A summary of the computation steps for the EKF using a state-space battery model is presented in Appendix I. This estimator executes the estimation of three of the 15 banks during a single iteration, requiring five iterations to finish the estimation of all 15 banks in the pack.

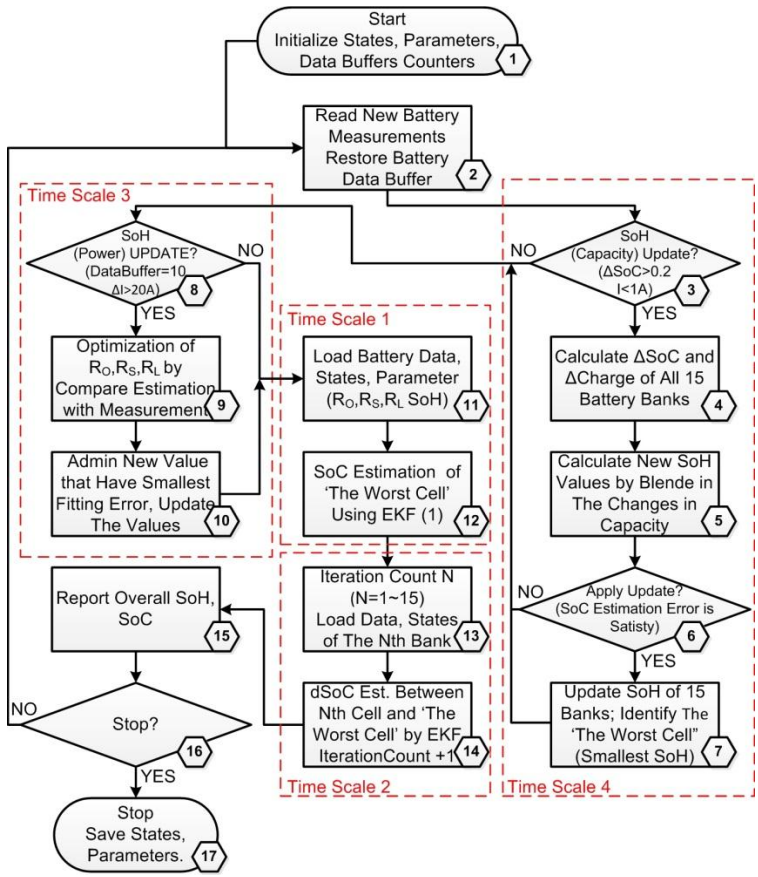

Figure 7. Flow chart of multiple time scales used for battery state estimation algorithm.

In Figure 8, four different computing time scales are compared under the same time line to illustrate how the estimation algorithms are carried out. As time is marched forward, the SoC of the worst bank is estimated in each time step (Time Scale 1). The SoCs of the rest of the banks are estimated with a larger time scale (Time Scale 2), which updates after every five iterations. The internal resistance value of the worst bank updates after every five iterations (Time Scale 3). Finally, the capacity of all 15 battery banks are updated after every 1000 iterations. Capacity degradation is a slow procedure and therefore uses the longest time steps to quantify its variation. Over all, the estimation tasks on different battery banks of different states are composed into one integrated scheme, where the computational iteration is matched to the dynamics of the each phenomenon.

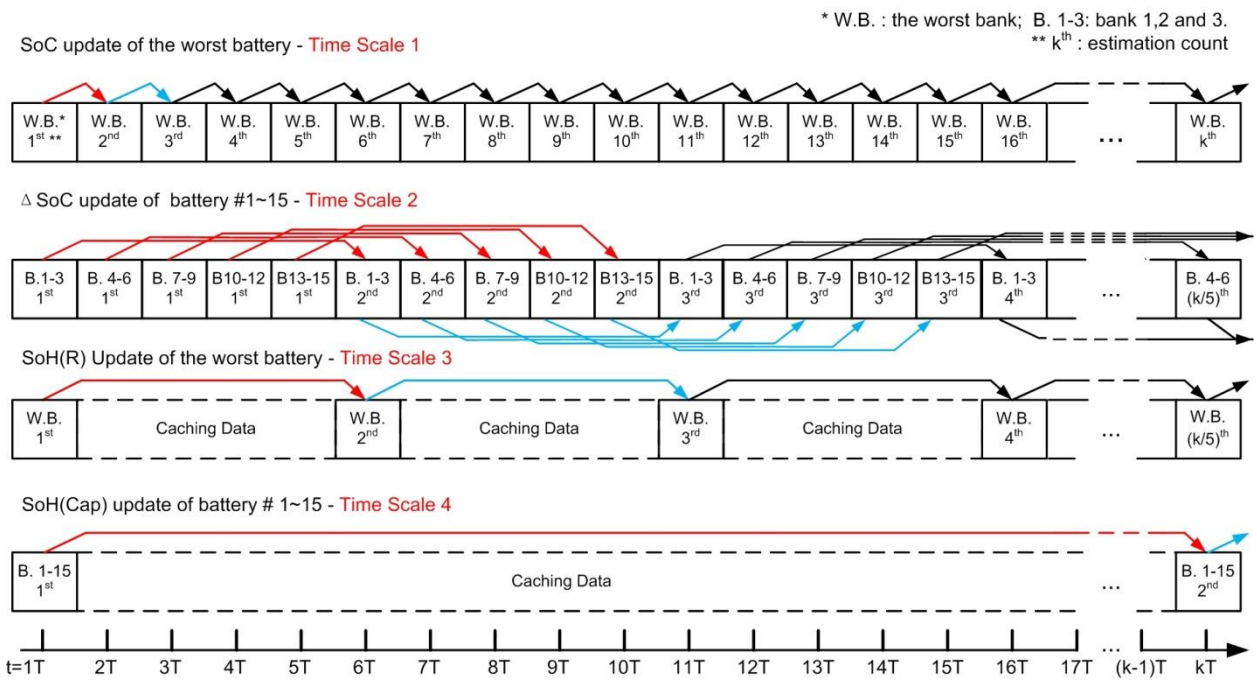

Figure 8. Diagram of multiple time scale battery state estimation algorithm.

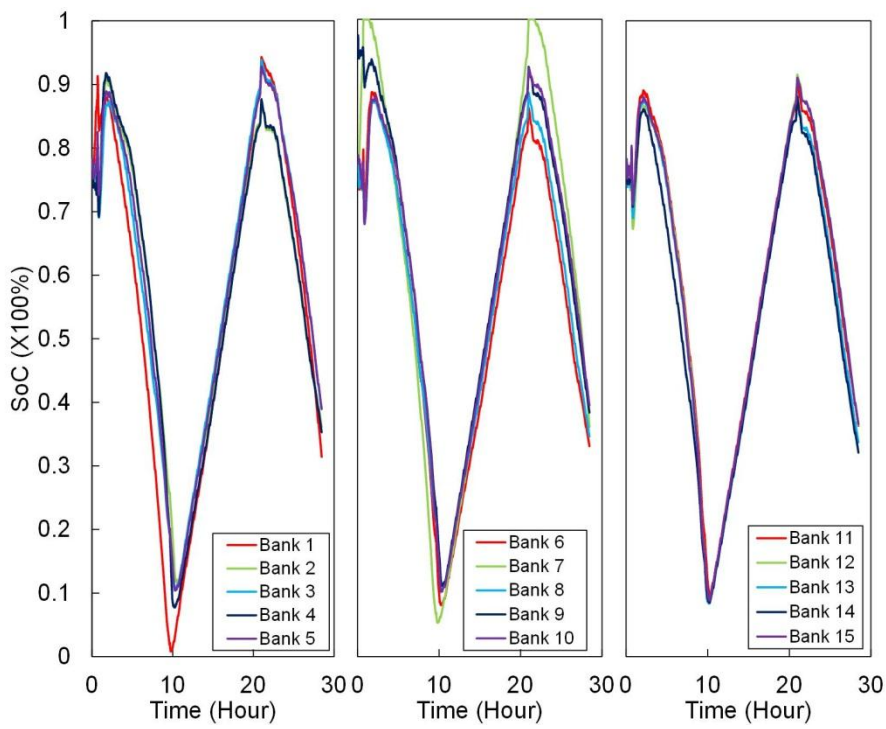

Figure 9. On-line battery SoC estimation during battery pack charge and discharge.

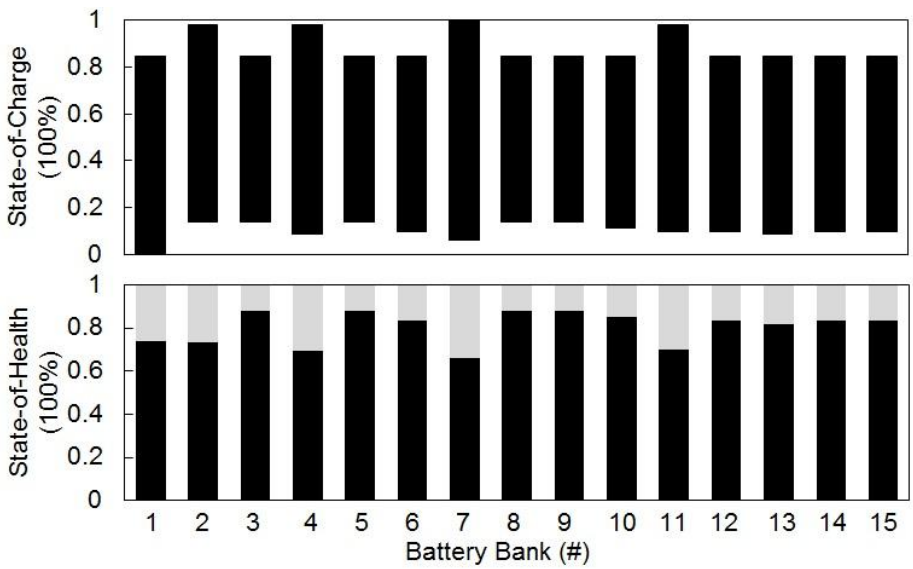

Figure 10: Identified battery pack SoC and SoH imbalance during system operation

Basic on-line estimation results are presented in Figure 9 and Figure 10. Applying the proposed battery management system, we are able to identify SoC and SoH of each individual battery bank. As shown in Figure 9, the battery estimation algorithm was able to estimate SoC of all 15 banks and successfully identify their differences during cycling. Figure 10 shows that the largest SoC difference among banks was about 10%, of which 5% will generally be compensated by the balancing circuits of the BMS and 5% was caused by SoH imbalance, which cannot been eliminated.

Energy Management Algorithm

The battery pack was operated as an energy buffer shifting energy from times of peak PV production to times of peak energy consumption. The battery charge versus discharge decision was made based on three system variables: 1) battery status, 2) time varying utility price, and 3) energy demand less the PV production. An example daily usage cycle typically has PV production occurring from 9am to 6pm, and any excess production will be stored in the battery pack. The typical energy usage peak occurs from 5pm to 9pm and typical utility time varying price peaks from 2pm to 8pm. During peak usage and peak utility price time periods, the battery tends to discharge to support the energy deficit. A detailed system energy flow management decision table is presented in Table 2, where row 1, 2 and 3 are input variables and row 4 is a list of system actions. This energy flow management approach is a mild strategy in terms of utilizing battery storage. When utility price is off peak, the energy demand will always be covered by the grid instead of battery.

A one day forecasting is also implemented in the algorithm. As shown in the Table 3, the battery SoC limits have a varying operation boundary condition: target SoC. This target SoC value marks the level of charge the battery pack should maintain at the end of the day. It is calculated every day at the evening when PV energy production is finished using the following equation:

$$SoC_{Target} = 60\% - 0.5 * \Delta SoC_{Batt} \quad (1)$$

where, SoC_{Target} is the target SoC at the end of the day (23:00), and ΔSoC_{Batt} is the variation of the battery SoC during the day (from dawn to 18:00). During the utility peak time, the battery pack will discharge to support the house load, but will not exceed the target SoC level, so that it will keep a good level of charge and also leave enough capacity for receiving excess energy production from the PV on the following day.

Table 2. Energy management decision making table.

Input 1	T	F	N	T	F	N	T	F	N	T	F	N	T	F	N	T	F	N
Input 2	T	T	T	F	F	F	T	T	T	F	F	F	T	T	T	F	F	F
Input 3	T	T	T	T	T	T	F	F	F	F	F	F	N	N	N	N	N	N
Action	F	C	F	D	S	D	F	C	C	D	S	S	F	C	C	D	S	S

Input
1:UtilityPrice T :Peak Price, N: Partial Peak, F: Off Peak
2:PVvs.Load T :PV product > Demand, F: PV product < Demand
3:BattSoC T : 90%~100%, N: Target SoC*~90%, F: 0%~Target SoC*%
*Target SoC is the SoC level battery pack will maintain at the end of the day

Action
F: GRID BACK FEED; S: GRID SUPPLY;
C: BATTERY CHARGE; D: BATTERY DISCHARGE

Figure 11 and Figure 12 present three days of system operation during good solar harvesting days and bad solar harvesting days, respectively. The top plot shows PV power, house energy demand, and the time varying utility price. The bottom plot shows the battery variation in SoC and power. As Figure 11 indicates, in sunny weather from 8am to 5pm, PV production is larger than the energy demand of the house. From 9am to 10am about 2kWh of PV production was utilized to charge the battery pack when the utility price was low. From 10am to 5pm, excessive production of PV energy was sent back to the grid. From 5pm to 8pm, about 3kWh of energy was provided by the battery pack to support the house energy demand during the peak utility price. Occasionally, the battery pack needs to be charged by the utility to bring the SoC to an appropriate level by the end of the day. As Figure 12 indicates, in rainy days, the daytime PV production was too low to support energy demand of the house. The battery discharged during the daytime, and was able to provide about 3kWh of energy during the peak utility pricing time period. The battery pack was charged up using off peak electricity during the nighttime, to maintain the target SoC. Overall, the battery pack plays a roll of supporting the house energy demand when the utility price is high. The proposed management algorithm cycles the battery pack with about 2kWh throughput per day, or 20% of the present battery capacity. The results indicate that by using at least 2kWh of battery pack capacity, a single family house can avoid peak usage of electricity, which greatly contributes to the grid stability. To further study the system, the research team will optimize the system size to bring down the cost. On the other

hand, some aggressive management algorithms will be investigated in which deeper cycling of the battery may be performed for grid respond and/or more peak shifting.

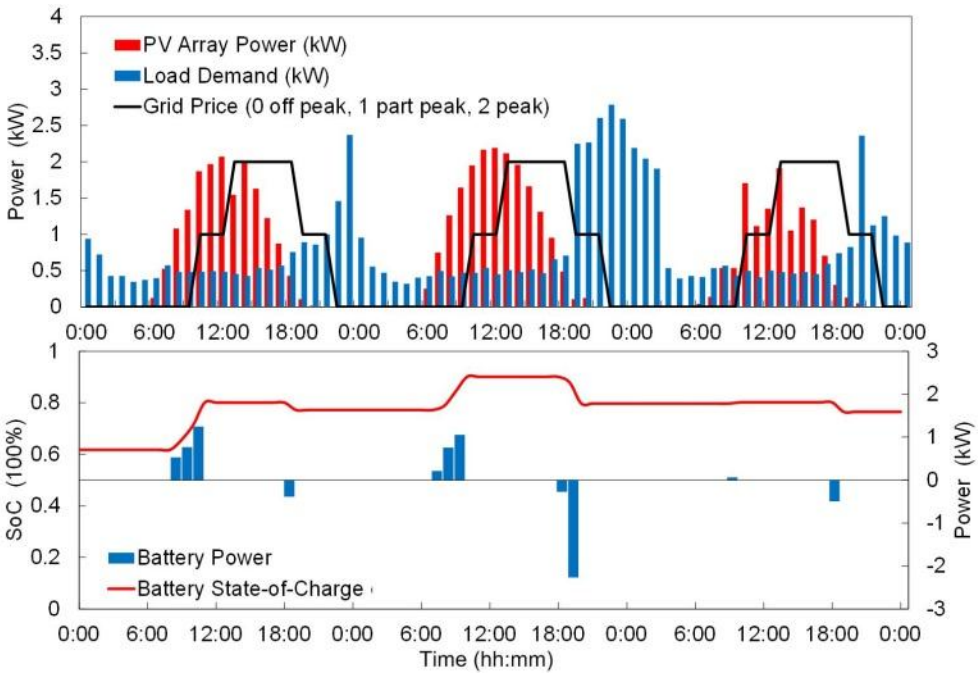

Figure 11. System operation simulation under good solar harvesting weather.

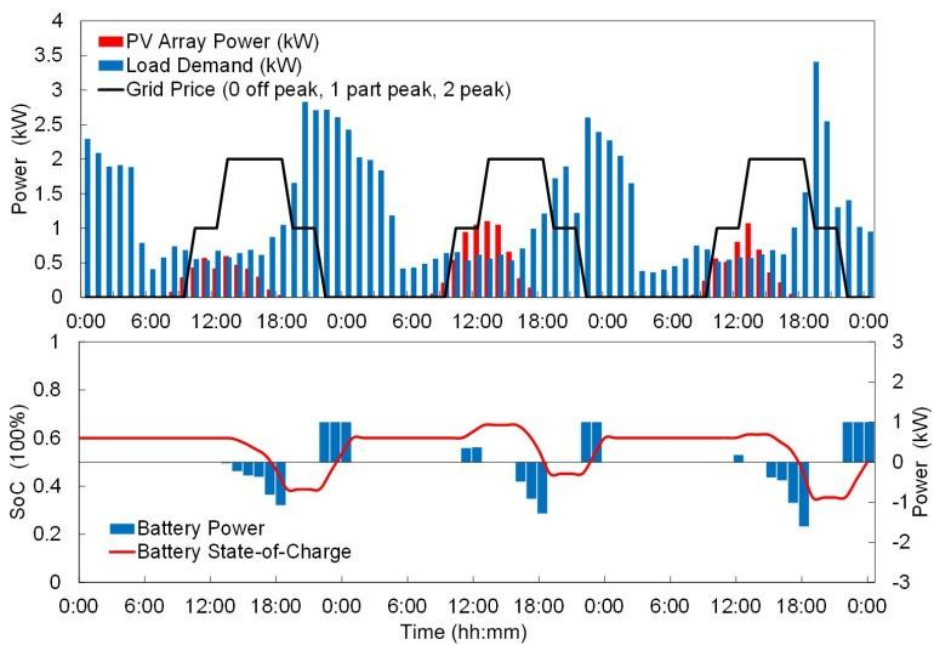

Figure 12. System operation simulation under poor solar harvesting weather.

System Design Document, Installation and Commissioning

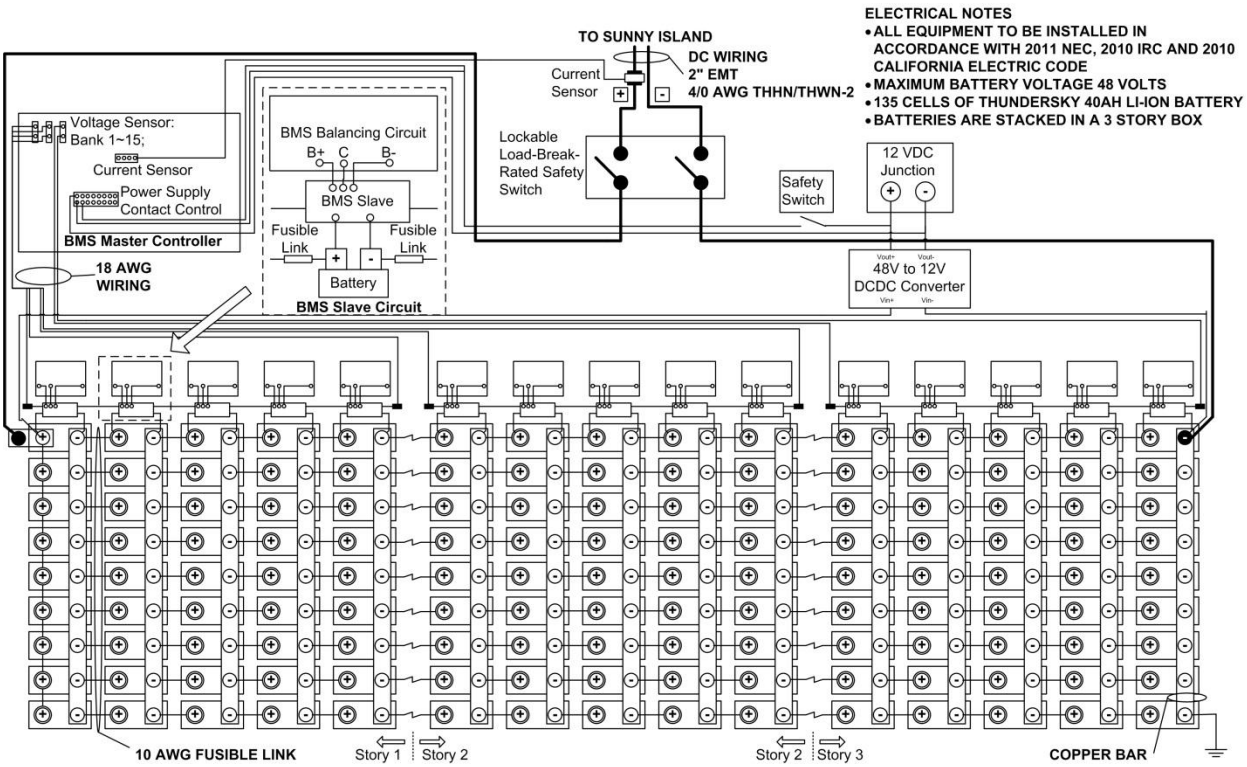

Figure 13. Design document – battery pack.

Based on the system design, the research team finalized the design documents. Figure 13 presents the finalized electrical schematic of the battery pack. Figure 14 presents the electrical schematic of the rooftop solar array with a DC junction box. Figure 15 presents the overall system electrical schematic, including one PV array, one battery pack, one vehicle charger, one Sunny Boy PV inverter, two Sunny Island battery inverters, one main electrical panel, one 240V AC panel for vehicle charger, one 48V DC panel for battery, and two 120V AC junction box for the battery inverter.

The design documents, along with the site plan, were submitted for university, city of Davis, and the fire marshal to gain permit approval. An electrical contractor was hired to collaborate with the research team to install all of the appliances into the house according to the plan. Over a period of two months all of the components were installed and tested to be functioning. A stitched photo is presented in the Figure 16, showing the primary system components after installation. PV panels were installed at rooftop. A smart meter and a smart panel were installed on the side wall of the house. The garage space is where the battery box, battery and PV inverters, junction boxes and breakers were installed.

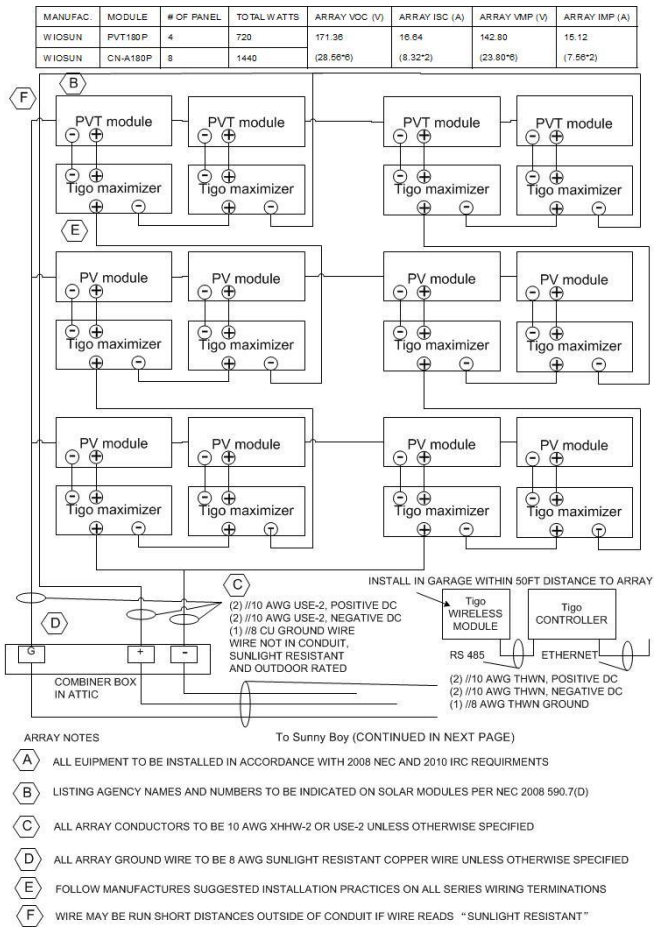

Figure 14: Design document – rooftop PV/PVT array.

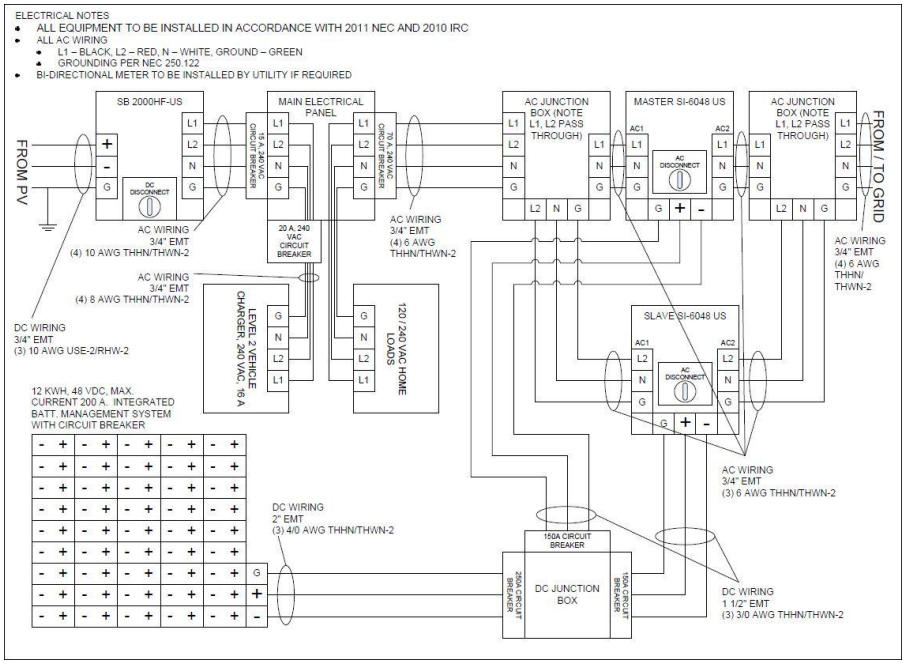

Figure 15. Design document– the overall energy system.

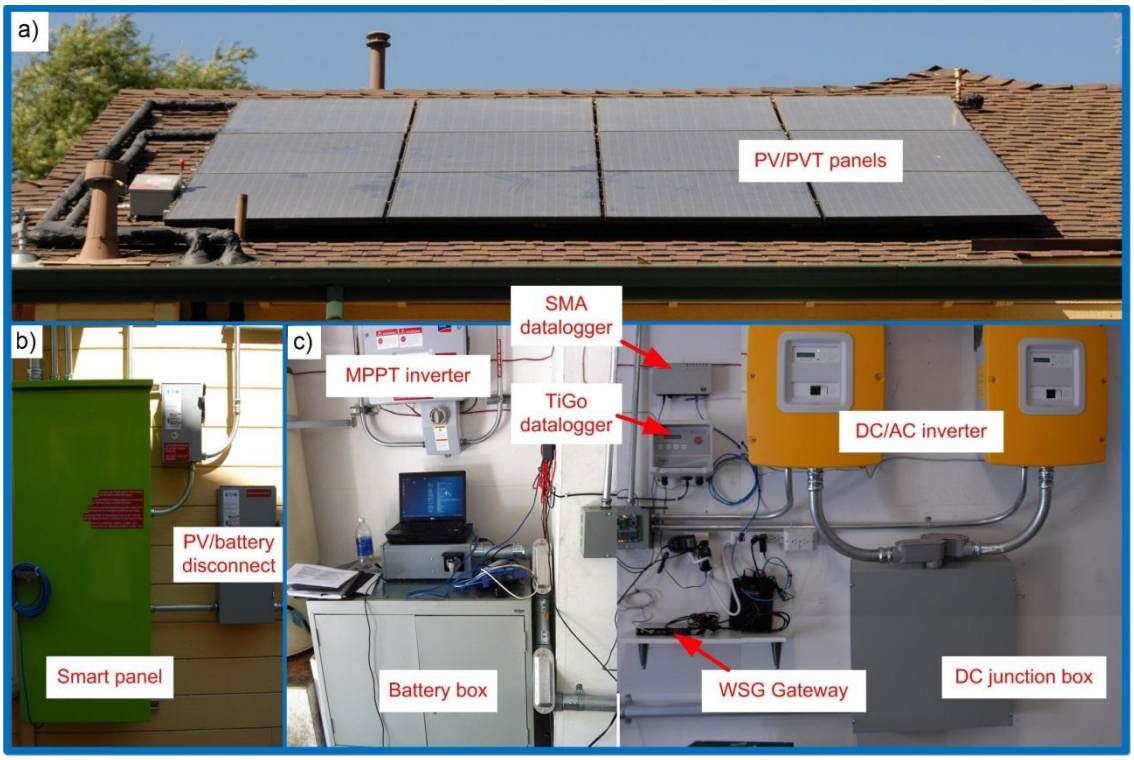

Figure 16. Photo of installed smart-grid PV battery system.

Remote Data Acquisition and Monitoring

An intelligent information network was installed for data collection and analysis. As illustrated in Figure 17, a WirelessGlue™ gateway serves as the central gateway that receives information from the battery management system (BMS), SMA®Webbox, Tigo® gateway, and ZigBee radios. The SMA®Webbox logs data of the SMA products, including the DC input from the battery pack, the AC output from the battery charger/discharger, and the AC output from the SMA MPPT PV converter. It also hosts a local HTTP server that can be continuously accessed through the central gateway (Line 4 in Figure 17). Similarly, the Tigo® gateway logs output data of each PV panel and transfers the data via wireless communication to the central gateway (Line 7). ZigBee radios connected to the central gateway via Ethernet were installed in the house. They receive data from ZigBee equipped appliances such as smart plugs, smart meter, and a ClipperCreek® vehicle charger (Line 5 and Line 6). The BMS receives voltage, current, and temperature measurements of each battery bank through Line 1, and estimates battery state-of-charge (SoC) and state-of-health (SoH) of the battery pack. Also, the BMS obtains the system operating data from the central gateway, including instant utility price, PV output, and house power demand. Based on the information, the BMS algorithm implements the design control decision, which is submitted to the central gateway (Line 2) and routed to the battery charger/discharger (Line 4) to operate the battery pack. Finally, the central gateway assembles all the data from different sources and sends the packaged system information to a server in the cloud.

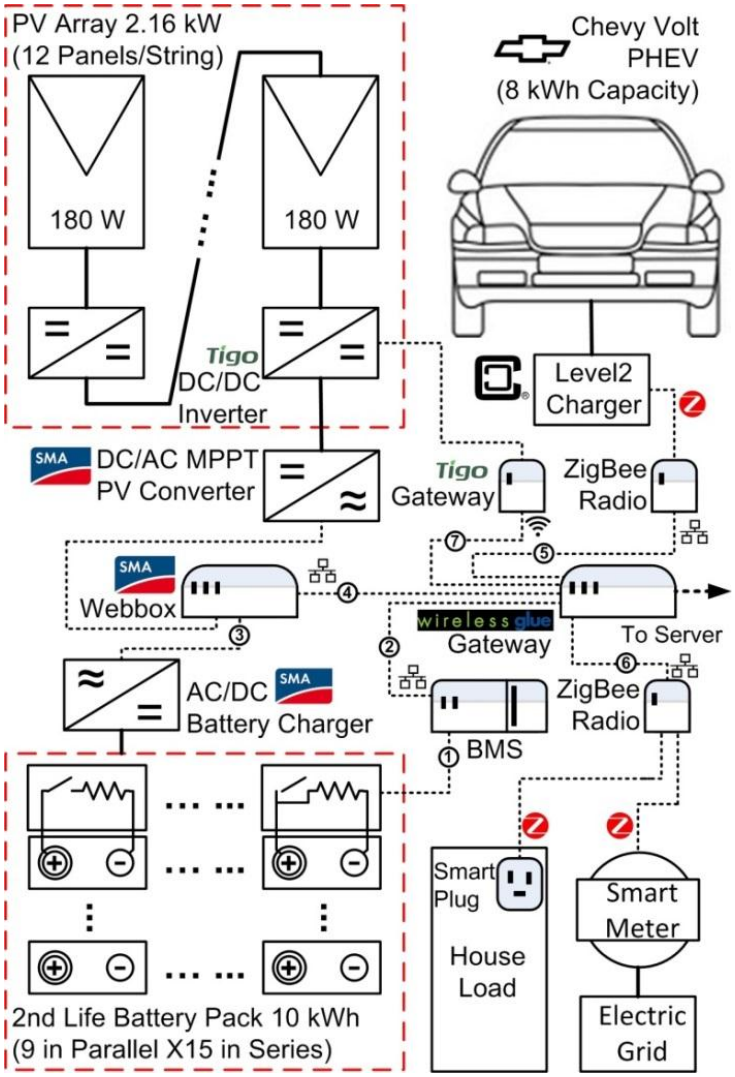

Figure 17. Diagram of system information network.

Table 3 lists the servers the research team developed for data logging. The main Aggie Village Home Server is run at the WirelessGlue gateway providing a host for the BMS and stores data on the local database. The Tigo and SMA sever logs PV energy data. The Obvius smart panel server logs grid interaction data. The battery data server logs battery operation data. Figure 18 shows a screen shot of the different data logging servers. In addition, a live data webpage was developed to monitor the PV, battery and grid operation with 24 hour data display and 7 days summation. A screen shot of the live data web page is shown in Figure 19. In addition, WirelessGlue provided the ZigBee data logger service to monitor the smart plug and ZigBee equipped appliance such as the vehicle charger. As a result, energy consumption of major appliances in the house can be individually monitored. This integrated information network allows researchers to keep good track of energy flow in the system. More importantly, it provides a convenient access for the users to check, manage and conserve their energy usage.

Table 3. List of data logging server

	Data Acquisition Service	Access
1)	Aggie Village Home Server via SSH protocol	ssh gsf@ucdavisvillage.no-ip.biz
2)	Tigo Energy via Tigo live view service	http://www.tigoenergy.com/
3)	SMA webbox server	http://ucdavisvillage.no-ip.biz:3334/
4)	Obvius smart panel server	http://ucdavisvillage.no-ip.biz
5)	Battery data server via FTP	FTP://ucdavisvillage.no-ip.biz
6)	Live data webpage	http://ucdavisvillage.no-ip.biz:9000/

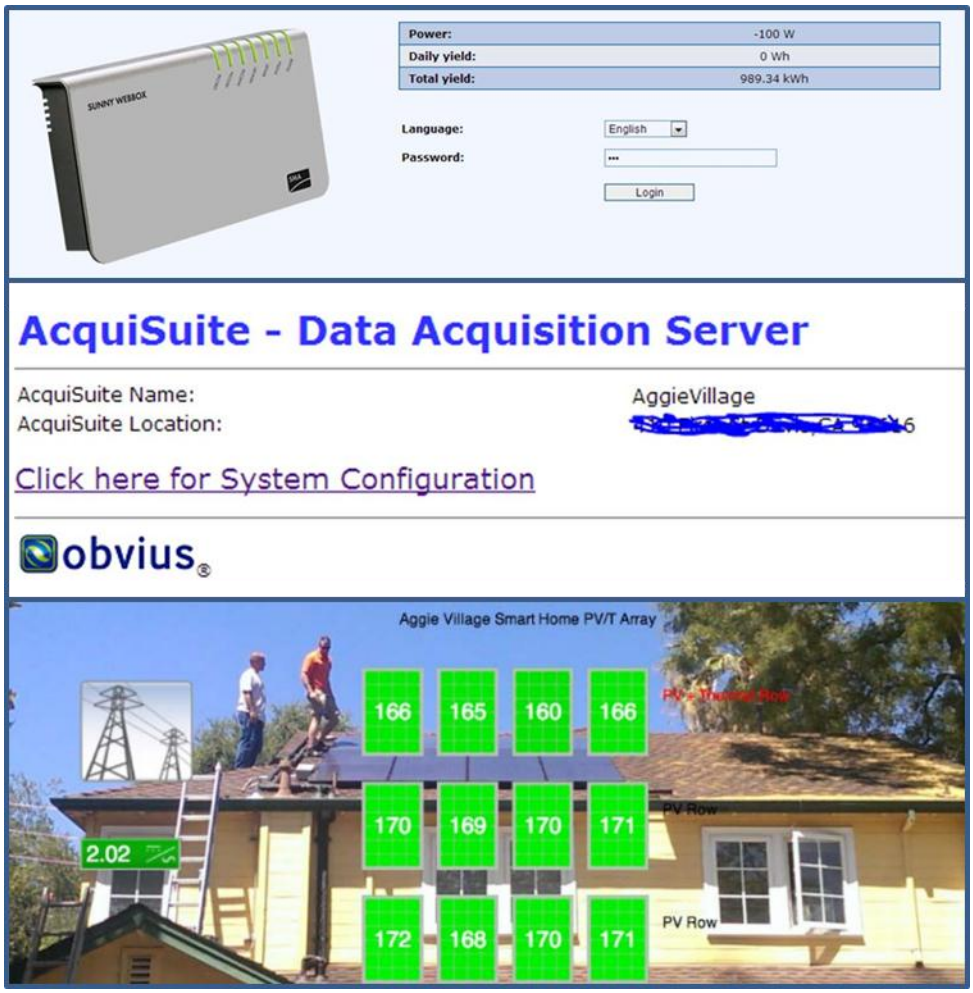

Figure 18: Screen shot of web based data server: top, SME Webbox; middle, Obvius smart panel; bottom, TiGo system

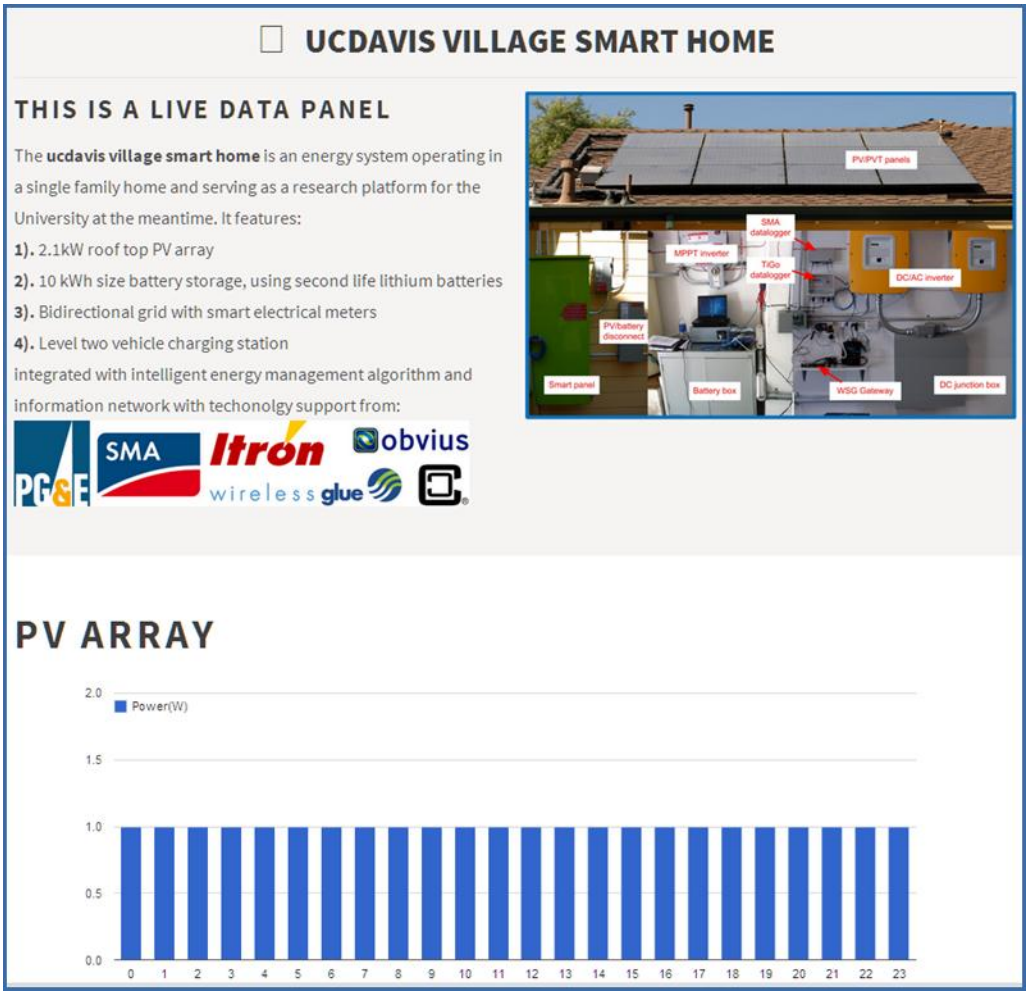

Figure 19. Screen shot of web based live data panel.

Results and Discussion

The system has been fully functioning with the data logger recording the usage history. Due to the reduced sun exposure in the winter, the PV system is outputting energy between 4 to 7kWh per day on good weather. Figure 21 shows a PV production summary from 11/19/2013 to 12/30/2013. Note that on certain days the energy output is less than 1kWh, which is due to a communication malfunction on the TiGo Solar Maximizer, resulting in zero production from one of the PV panels on occasion. This issue was resolved on January 21st 2014. Aside from that, the PV array is working properly.

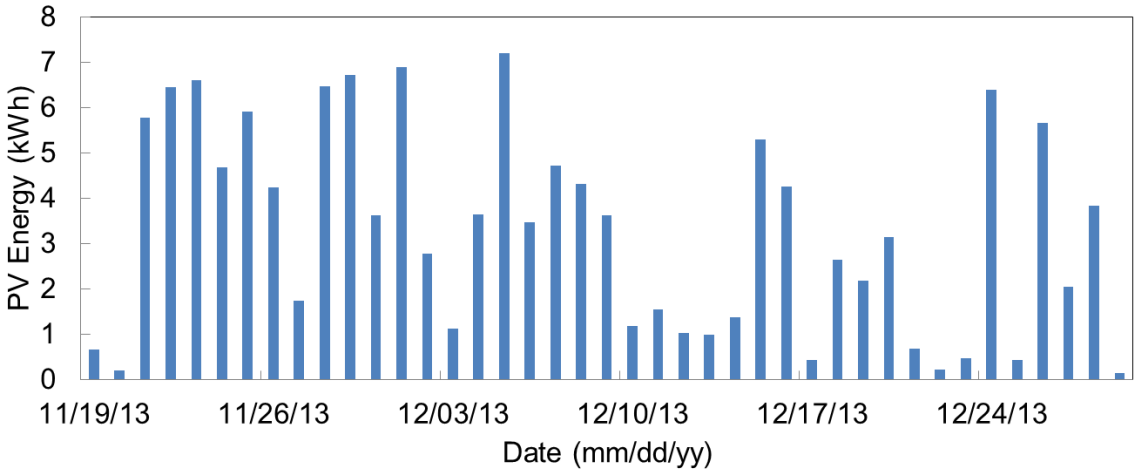

Figure 20. Daily PV Array Energy Harvesting Summary (11/19/2013 to 12/30/2013).

Over the course of the first four months of PV array operation 967kWh energy was produced. Equivalent CO2 saving equals to 1639 lbs. The battery system starts to function from late November 2013, and over the one month it performed PV energy shifting of 63 kWh, equivalent to US$18.9 saving. It prolonged the battery second life by 11 cycles. Over all the system has saved US$145.5 over the first four months in winter time operation.

Table 4. System operation statistics.

PV System (09/2013 to 12/2013)	Operation Hours (system on)	1483 Hours
	Energy Harvested	967 kWh
	CO2 Saved	1639 lbs.
Battery Pack (11/2013 to 12/2013)	Peak Usage Shifted	63 kWh
	Peak Usage Bill Saved (@0.3$/kWh)	18.9 $
	Extended Battery Life	11 Cycles
Grid Interaction (09/2013 to 12/2013)	Electricity Bill Saved (@0.15$/kWh)	145.5 $

The system provides a renewable energy source when solar energy is available in the daytime and covers part of the load in the night using the reserved energy in the battery. **Error! Reference source not found.** illustrates the system functionality using usage data on December 1st, 2013. As shown in **Error! Reference source not found.**, from midnight to 10am both the PV array and battery pack were in silent mode. The house energy usage was fully supported by the grid. From 10am to 5pm, the house energy demand was fully supported by the PV array output and the excess energy of the PV was used to charge the battery. From 5 pm to 8 pm, the house energy usage peak arrived, overlapping with the utility peak pricing hour. The battery discharges to support the load demand with an efficiency of approximately 85%. When the peak pricing finished after 8pm, the battery stopped discharging. As shown in the energy consumption pie chart in the Figure 21, the house energy demand in that day consisted of 30% peak pricing usage (3.2kWh), 20% partial peak usage (2.4kWh), and 50% off peak usage (5.7kWh). Indicated by the energy source pie chart, 63% of the house energy usage was covered by the PV array production (6.8kWh). With the battery pack enabled peak shifting, the peak usage during the nighttime is covered by the stored PV energy (3kWh) in the battery.

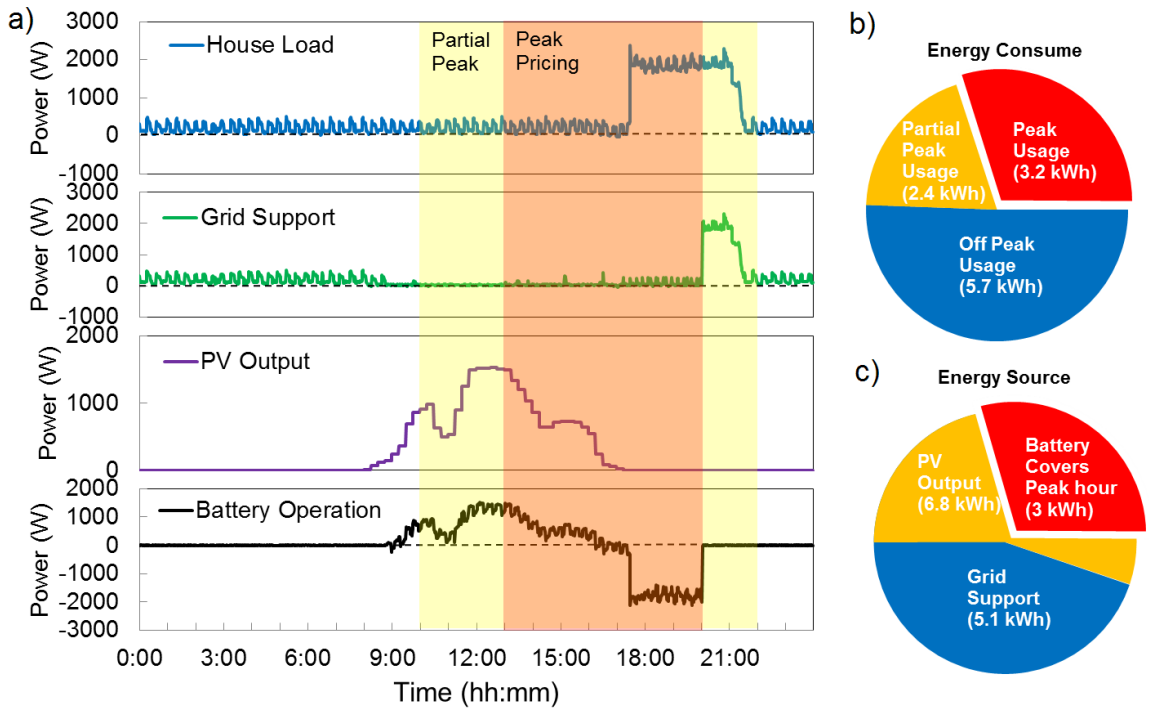

Figure 21. Sample of system operation on 11/29/2013. a) Plots of power draw and supply over an entire day. b) Pie chart of energy consumption broken down based on price of usage. c) Energy supplied as a function of the source.

On a different day of operation (November 29th, 2013), a slightly different energy management algorithm was utilized. At peak hours, instead of charging the battery, the PV output was fed back to the grid. As shown in Figure 22, from midnight to 10am, both the PV array and battery pack were in silent mode. The house energy usage was fully supported by the grid. From 10am to 5pm, the house energy demand was supported by both the PV and grid. When the PV output was higher than the house demand, excessive energy of the PV was used to charge the battery. From 5pm to 8pm, the house energy usage peak arrived, the battery discharged to support the load demand with an efficiency near 85%. At the same time, the PV supported the energy demand with the remaining sunlight. Any excessive production was sent back to the grid. When the peak pricing finished at 8pm, the battery stopped discharging. As shown in the energy consumption pie chart in Figure 22, the house energy demand in that day consisted of 17% peak pricing usage (3.2kWh), 47% partial peak usage (8.4kWh), and 35% off peak usage (6.4kWh). Indicated by the energy source pie chart, 63% the house energy usage was covered by the PV array production (7.2kWh). With the battery pack enabled peak shifting, the peak usage during nighttime was covered by the PV energy or battery stored PV energy (0.9kWh form direct PV energy, 0.9kWh from battery discharge energy). Using this energy management strategy, the PV energy was sent back to the grid to obtain more optimal economics. Meanwhile the battery usage was less. The energy system operated by this strategy can have a smaller size battery pack, but will have a larger grid dependency.

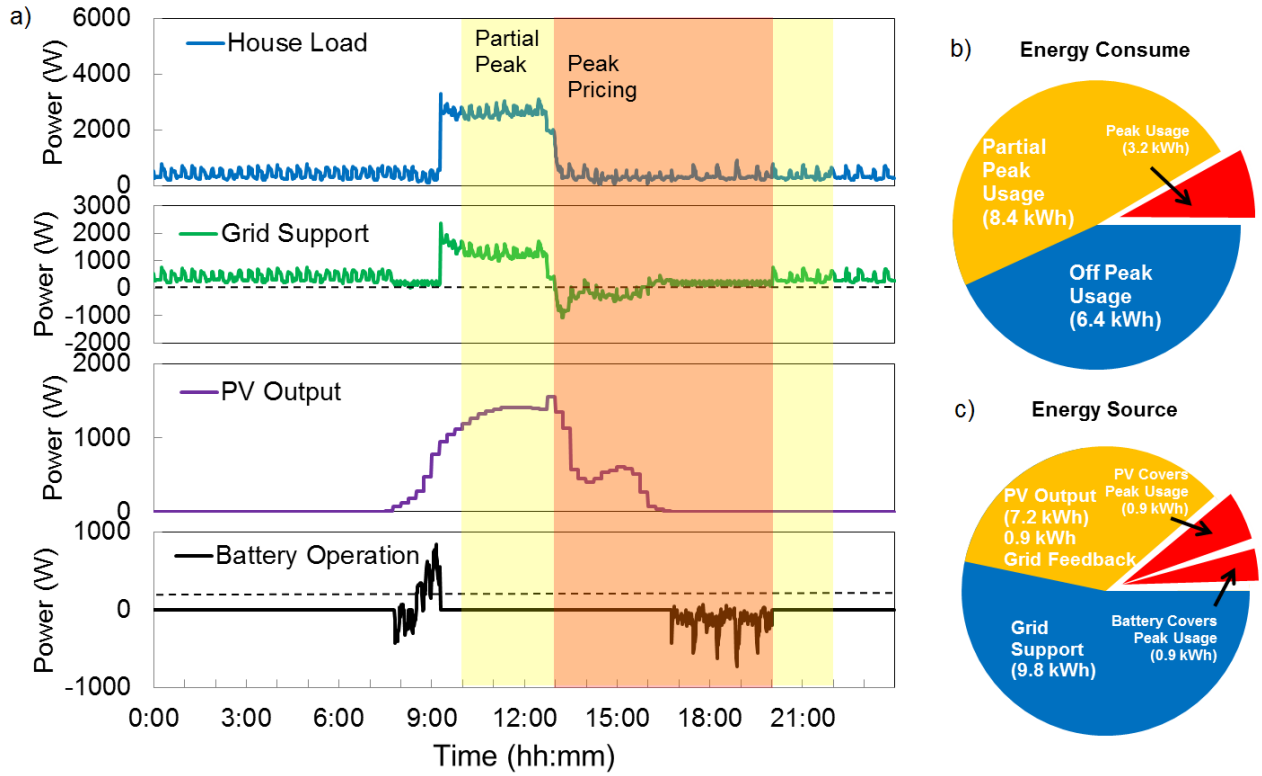

Figure 22. Sample of system operation on 12/10/2013. a) Plots of power draw and supply over an entire day. b) Pie chart of energy consumption broken down based on price of usage. c) Energy supplied as a function of the source.

Conclusions

The Research team of task 1.2 supervised by Dr. Jae Wan Park has successfully delivered a smart energy system equipped with: 1) renewable high efficiency PV/PVT array; 2) smart grid enhanced utility interaction; 3) battery storage featuring second life vehicle traction battery application for peak shifting and grid response; 4) level 2 vehicle charging station to promote PHEV ownership; and 5) comprehensive data logging service for in-depth system analysis.

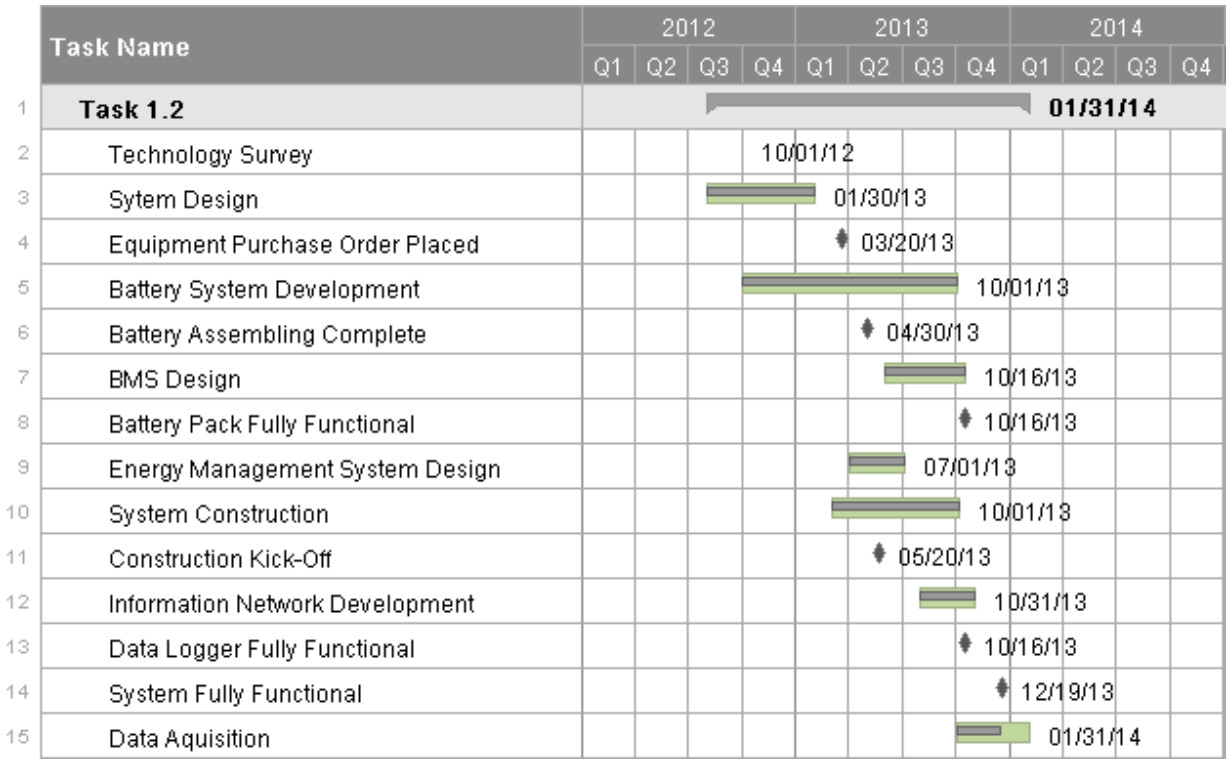

Figure 23: Summary of project roadmaps and milestones of Task 1.2

The system development has been completed at the project house, providing renewable energy to a single family, and meanwhile providing detailed data of energy system operation for research. The research team has followed the project roadmap (Figure 23), and fulfilled periodical milestones. The resulting system meets all the proposed functionality.

Recommendations

California has set an ambitious goal of having 33% of its electricity generation to be provided by renewable sources. Due to the instabilities of wind and solar energy storage will be an important component to enabling the meeting of this target. Energy storage enables the stable use of renewables for peak shaving, which can dramatically reduce the overall pollution caused by electricity generation as this is the critical period in which "peaker" plants, which generate the highest level of emissions, are operated. Finally, applying the use of second life lithium ion batteries for renewable storage have great potential when applied as distributed energy storage solutions at the site of renewable generation, for example when applied to residential homes as performed on this project.

As mentioned above the use of renewables has a critical impact on grid stability, however, the cost of energy as well as the prediction of grid demand also have certain levels of uncertainty associated with them. Employing energy storage into the grid can enable response to changing supply and demand at rates significantly improved over current state of the art techniques. With improved demand response, the possibility of Brown-outs or Black-outs may even be banished entirely, a dramatic benefit to the California public after they faced these issues first hand in the early 2000's.

References

1. Agency, International Energy. "Trends in Photovoltaic Applications: Survey Report of Selected Iea Countries between 1992 and 2009.". (2010).
2. Bragard, M., N. Soltau, S. Thomas, and R. W. De Doncker. "The Balance of Renewable Sources and User Demands in Grids: Power Electronics for Modular Battery Energy Storage Systems." Power Electronics, IEEE Transactions on 25, no. 12 (2010): 3049-56.
3. Doughty, Daniel H, Paul C Butler, Abbas A Akhil, Nancy H Clark, and John D Boyes. "Batteries for Large-Scale Stationary Electrical Energy Storage." The Electrochemical Society Interface (2010): 49-53.
4. Duryea, S., S. Islam, and W. Lawrance. "A Battery Management System for Stand-Alone Photovoltaic Energy Systems." Industry Applications Magazine, IEEE 7, no. 3 (2001): 67-72.
5. Ekren, O., and B. Y. Ekren. "Size Optimization of a Pv/Wind Hybrid Energy Conversion System with Battery Storage Using Simulated Annealing." [In English]. Applied Energy 87, no. 2 (Feb 10 2010): 592-98.
6. Ferreira, Summer , Wes Baca, Tom Hund, and David Rose. "Life Cycle Testing and Evaluation of Energy Storage Devices." ESS Peer Review Sandia National Laboratories (2012).
7. Haihua, Zhou, T. Bhattacharya, Tran Duong, T. S. T. Siew, and A. M. Khambadkone. "Composite Energy Storage System Involving Battery and Ultracapacitor with Dynamic Energy Management in Microgrid Applications." Power Electronics, IEEE Transactions on 26, no. 3 (2011): 923-30.
8. Hill, C. A., M. C. Such, Chen Dongmei, J. Gonzalez, and W. M. Grady. "Battery Energy Storage for Enabling Integration of Distributed Solar Power Generation." Smart Grid, IEEE Transactions on 3, no. 2 (2012): 850-57.
9. Hund, Tom , Nancy Clark, and Wes Baca. "Testing and Evaluation of Energy Storage Devices." ESS Peer Review Sandia National Laboratories (2008).
10. Jacobson, M. Z. "Review of Solutions to Global Warming, Air Pollution, and Energy Security.". Energy & Environmental Science 2, no. 2 (2009): 148-73.
11. Landgrebe, Albert R., and Samuel W. Donley. "Battery Storage in Residential Applications of Energy from Photovoltaic Sources." Applied Energy 15, no. 2 (// 1983): 127-37.
12. Neubauer, J., and A. Pesaran. "The Ability of Battery Second Use Strategies to Impact Plug-in Electric Vehicle Prices and Serve Utility Energy Storage Applications." . Journal of Power Sources 196, no. 23 (Dec 1 2011): 10351-58.
13. Omran, W. A., M. Kazerani, and M. M. A. Salama. "Investigation of Methods for Reduction of Power Fluctuations Generated from Large Grid-Connected Photovoltaic Systems." Energy Conversion, IEEE Transactions on 26, no. 1 (2011): 318-27.
14. Ongaro, F., S. Saggini, and P. Mattavelli. "Li-Ion Battery-Supercapacitor Hybrid Storage System for a Long Lifetime, Photovoltaic-Based Wireless Sensor Network." Power Electronics, IEEE Transactions on 27, no. 9 (2012): 3944-52.
15. Rydh, C. J., and B. A. Sanden. "Energy Analysis of Batteries in Photovoltaic Systems. Part Ii: Energy Return Factors and Overall Battery Efficiencies.". Energy Conversion and Management 46, no. 11-12 (Jul 2005): 1980-2000.

16. Samaras, Constantine, and Kyle Meisterling. "Life Cycle Assessment of Greenhouse Gas Emissions from Plug-in Hybrid Vehicles: Implications for Policy." Environmental Science & Technology 42, no. 9 (2008/05/01 2008): 3170-76.
17. Schoenung, Susan. "Energy Storage Systems Cost Update." SAND2011-2730 (2011).
18. Tong, Shi Jie, Adam Same, Mark A Kootstra, and Jae Wan Park. "Off-Grid Photovoltaic Vehicle Charge Using Second Life Lithium Batteries: An Experimental and Numerical Investigation." Applied Energy 104 (2013): 740-50.

Appendix

Appendix I. Summary of EKF for battery SoC and deltaSoC estimation

The battery pack have 15 banks in serial, each requires individual estimation of its SoC. A worst-difference estimation using EKF was developed for this task. Table 5 presents the state-space model used for the worst battery bank. Table 6 presents the state-space model of the rest of the bank in comparison of the worst battery bank. Table 7 presents the computational steps used by the nonlinear extended Kalman filter

---

Computes each iteration Δt =5s

State and parameter variables

$$x = [SoC, U_S, U_L], \qquad P = [R_S(1 - exp(\frac{-\Delta t}{R_S C_S})), R_L(1 - exp(\frac{-\Delta t}{R_L C_L})), R_{Ohmic}]$$

Functions

$$f(x_k, u_k, \mathrm{P}_k) = Ax + \begin{bmatrix} P(1) \\ P(2) \end{bmatrix} I$$

$$g(x_k, u_k, \mathrm{P}_k) = OCV(SoC) + U_S + U_L + P(3)I$$

where

$$A_k = \begin{bmatrix} 1 & 0 & 0 \\ 0 & exp(\frac{-\Delta t}{R_S C_S}) & 0 \\ 0 & 0 & exp(\frac{-\Delta t}{R_L C_L}) \end{bmatrix}, \qquad C_k = \begin{bmatrix} \left.\frac{dOCV(SoC)}{SoC}\right|_{SoC = So\hat{C}_k^-} & 1 & 1 \end{bmatrix}$$

$$C_k^P = \begin{bmatrix} 0 & 0 & 0 & I_k \end{bmatrix}$$

$$+\begin{bmatrix} \frac{dOCV}{dSoC} & 1 & 1 \end{bmatrix} \left\{ \begin{bmatrix} I_{k-1} & 0 & 0 & 0 \\ 0 & I_{k-1} & 0 & 0 \\ 0 & 0 & I_{k-1} & 0 \end{bmatrix} + \begin{bmatrix} 1 & 0 & 0 \\ 0 & exp(\frac{-\Delta t}{R_S C_S}) & 0 \\ 0 & 0 & exp(\frac{-\Delta t}{R_L C_L}) \end{bmatrix} \left(-L_{k-1}^x \begin{bmatrix} 0 & 0 & 0 & I_{k-1} \end{bmatrix} \right) \right\}$$

Initialize with

$$\Sigma_w = [1; 0.0001; 0.001], \Sigma_v = 10, \Sigma_r = 0, \Sigma_e = 0$$

note that parameters other than P is not time varying; $\tau_S = R_S C_S = 5$, $\tau_L = R_L C_L = 50$

Table 5: Summary of state-state model for the worst battery bank

For cell number k=1,…15, computes every 15 iteration Δt =75s

State and parameter variables

$$x = \Delta SoC, \qquad P = \frac{\Delta t}{C_{NOM} SoH}$$

Functions

$$f(x_k, u_k, \mathrm{P}_k) = Ax + \begin{bmatrix} P & -\frac{\Delta t}{C_{NOM} SoH_{ref}} \end{bmatrix} \begin{bmatrix} I \\ I_{ref} \end{bmatrix}$$

$$g(x_k, u_k, \mathrm{P}_k) = OCV(x + SoC_{ref}) - OCV(SoC_{ref})$$

Where

$$A_k = 1, \qquad C_k = \left. \frac{dOCV(SoC)}{dSoC} \right|_{SoC = \hat{SoC}_k^-}, \qquad C_k^P = C_k(I_k)$$

Initialize with

$$\Sigma_w = 1, \Sigma_v = 10, \Sigma_r = 0, \Sigma_e = 0$$

note that parameters other than P is not time varying

Table 6: Summary of state space model for the difference between the worst banks and the rest of the banks

Nonlinear state-space model

$$x_{k+1} = f(x_k, u_k, P_k) + w_k$$

$$y_k = g(x_k, u_k, P_k) + v_k$$

Definition

$$A_{k-1} = \left.\frac{\partial f(x_{k-1}, u_{k-1}, P_k)}{\partial x_{k-1}}\right|_{x_{k-1} = \hat{x}_{K-1}^{+}}, C_k = \left.\frac{\partial g(x_k, u_k, P_k)}{\partial x_k}\right|_{x_k = \hat{x}_K^{-}}$$

Initialize with

$$\hat{x}_0^{+} = E[x_0]$$

$$\Sigma_{x,0}^{+} = E[(x_0 - \hat{x}_{K-1}^{+})(x_0 - \hat{x}_{K-1}^{+})^{\mathrm{T}}]$$

Computation for $k \in \{1, \ldots, \infty\}$

State estimate time update:

$$\hat{x}_k^{-} = f(\hat{x}_{k-1}^{+}, u_k, \hat{P}_k^{-})$$

$$\Sigma_{\hat{x},k}^{-} = A_{k-1} \Sigma_{\hat{x},k-1}^{+} A_{k-1}^{T} + \Sigma_w$$

State estimate measurement update:

$$L_k^x = \Sigma_{\hat{x},k}^{-} (C_k^x)^T [C_k^x \Sigma_{\hat{x},k}^{-} (C_k^x)^T + \Sigma_v]^{-1}$$

$$\hat{x}_k^{+} = \hat{x}_k^{-} + L_k^x [\mathrm{y}_k - \mathrm{g}(\hat{x}_k^{-}, u_k, \hat{P}_k^{-})]$$

$$\Sigma_{\hat{x},k}^{+} = (I - L_k^x C_k^x) \Sigma_{\hat{x},k}^{-}$$

where w, v are independent, zero-mean, Gaussian noise processes of covariance Σ_w, Σ_v

Table 7: Summary of computation steps for Extended Kalman Filter.